Finite element simulation of ionic electrodiffusion in cellular geometries

Ada Johanne Ellingsrud

Math bio seminar
University of Pennsylvania, Philadelphia, USA
November 2022

simula waterscales EMIx erc Forskningsrådet
The Research Council of Norway

Classical models for excitable tissue assume that the domain can be represented in an homogenized manner

Technology now allows for numerical resolutions below model resolution.

$$v_t - \nabla\cdot(M_i\nabla v + M_i\nabla u_e) = -I_{\text{ion}},$$
$$\nabla\cdot(M_i\nabla v + (M_i + M_e)\nabla u_e) = 0,$$
$$s_t = F(v, s).$$

How to model spatial variations in membrane properties, or how cellular morphology affect the dynamics?

How to model a single cell or a small collection of cells?

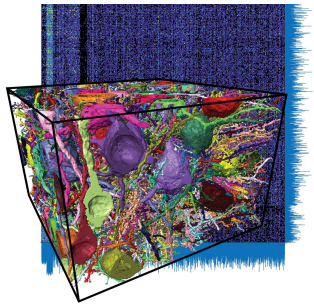

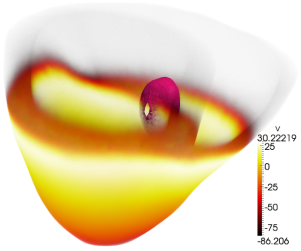

Physiological heart cell: $h \approx 100\mu$m
Computational mesh cell: $h \leq 100\mu$m

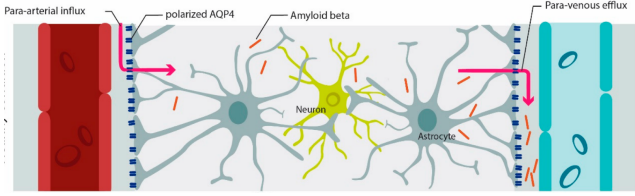

The emerging EMI framework use a geometrically explicit representation of the cellular domains

Find the intracellular and extracellular potentials $\phi_i = \phi_i(x, t)$ and $\phi_e = \phi_e(x, t)$, and the transmembrane current $I_M = I_M(x.t)$ s.t.:

$$-\nabla \cdot (\sigma_i \nabla \phi_i) = 0 \quad \text{in } \Omega_i, \tag{1}$$

$$-\nabla \cdot (\sigma_e \nabla \phi_e) = 0 \quad \text{in } \Omega_e, \tag{2}$$

$$\phi_M = \phi_i - \phi_e \quad \text{at } \Gamma, \tag{3}$$

$$\sigma_e \nabla \phi_e \cdot n_e = -\sigma_i \nabla \phi_i \cdot n_i = I_M \quad \text{at } \Gamma, \tag{4}$$

$$\frac{\partial \phi_M}{\partial t} = \frac{1}{C_M}(I_M - I_{\text{ion}}) \quad \text{at } \Gamma. \tag{5}$$

Ion concentrations are assumed to be constant in space and time – often an accurate approximation, but not always . . .

[Krassowska & Neu 1994],
[Ying & Henriquez 2007],
[Tveito et al. 2017]

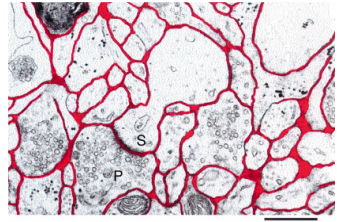

Rat cortex with ECS in red [Nicholson, 1998]

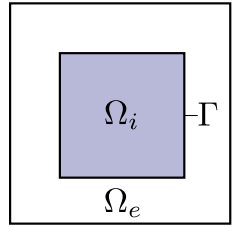

Outline

- Motivation and physiological background
- Modelling electrodiffusion: main assumptions and core ideas
- The KNP-EMI model: strong form and numerical strategies
  - Multi-dimensional form and a mortar finite element method
  - Single-dimensional form and a DG finite element method
- A study of ephaptic coupling
- Future perspectives

Brain tissue is composed of networks of extracellular spaces and primarily two classes of cells: neurons and glial cells

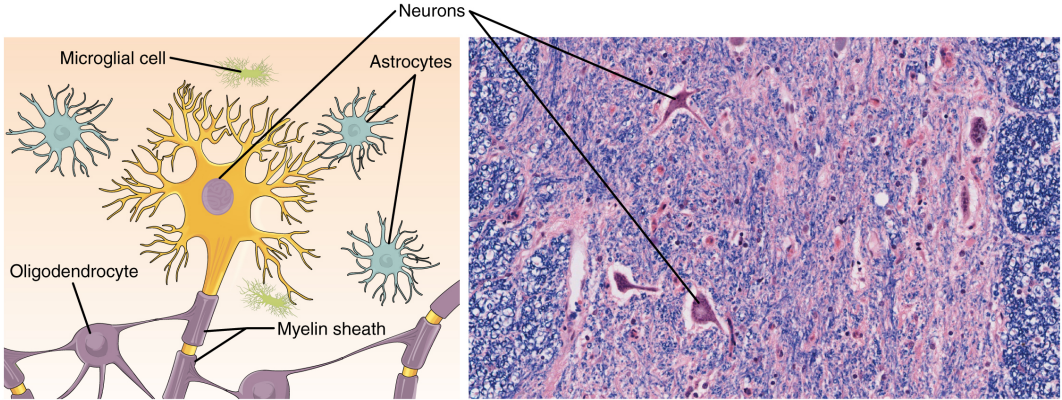

Left panel: Sketch of neurons and glial cells. Right panel: Micrograph of brain tissue. [OpenStax CNX, 2016]

Movement of ions is fundamental in brain signalling and various mechanisms ensure ionic homeostasis

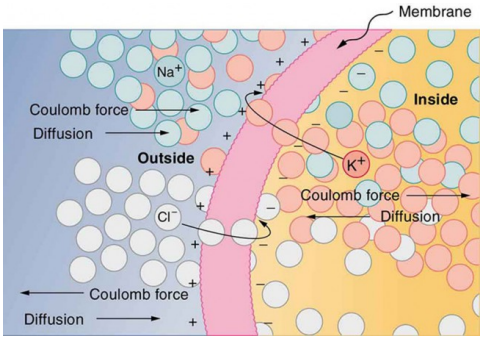

[courses.lumenlearning.com]

Movement of ions is fundamental in brain signalling and various mechanisms ensure ionic homeostasis

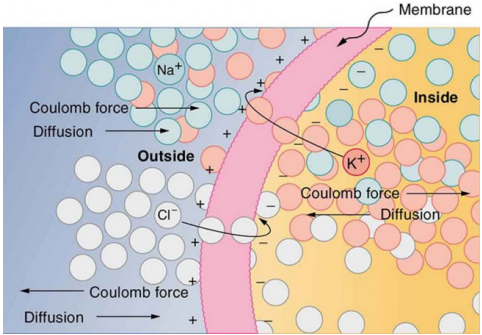

[courses.lumenlearning.com]

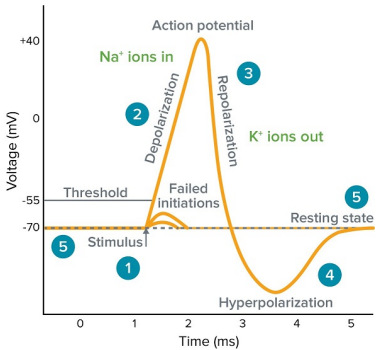

Movement of ions is fundamental in brain signalling and various mechanisms ensure ionic homeostasis

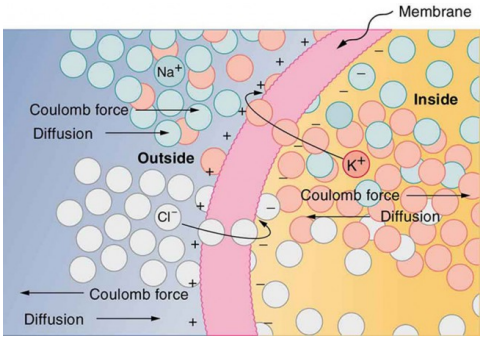

[courses.lumenlearning.com]

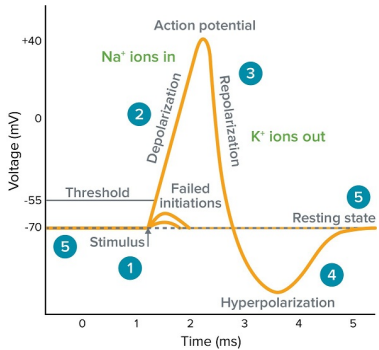

Homeostatic mechanisms will take the ionic concentrations back towards baseline levels, e.g.:

- Na^+/K^+/ATPase pumps (3 Na^+ out, 2 K^+ in),
- cotransporters (KCC2, NKCC1),
- glial K^+ buffering.

Ion concentration changes are a trademark of several pathological conditions, such as epilepsy or spreading depression

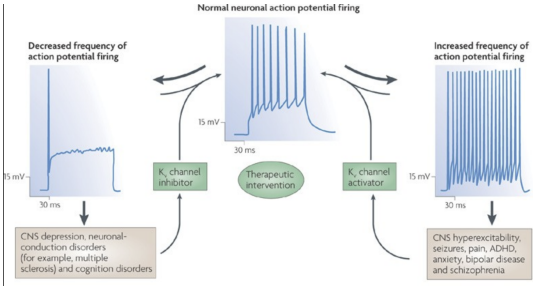

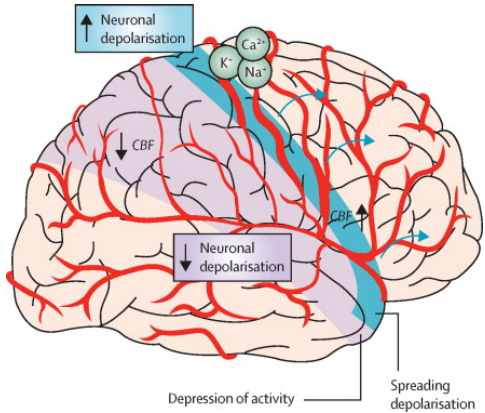

- Homeostatic mechanisms are not able to ”keep up”
- Shifts in the ECS ion concentrations

The extracellular ion composition changes with local neuronal activity and across brain states

Ionic shift may set up osmotic gradients causing cellular swelling.

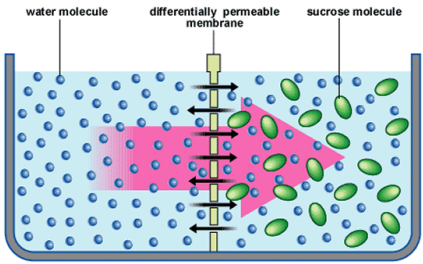

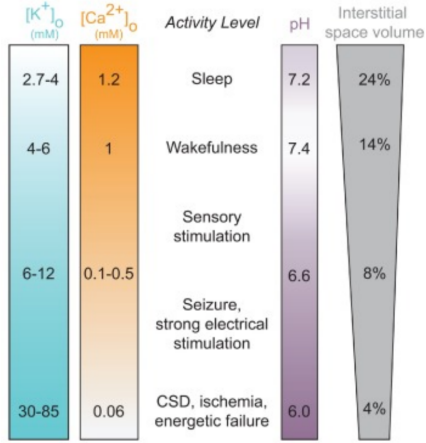

[Rasmussen, 2021]

Modeling electrodiffusion: main assumptions and core ideas

Electrodiffusion is governed by the Nernst–Planck equation, stating that ions move due to diffusion or drift in the electrical field

Diffusion

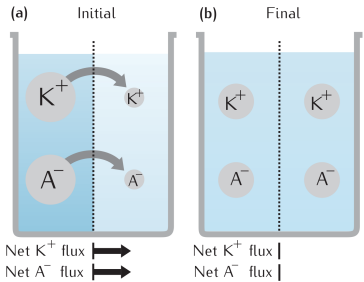

$$\mathbf{J}^k = \underbrace{-D^k \nabla [k]}_{\text{diffusion}}$$

Electrodiffusion is governed by the Nernst–Planck equation, stating that ions move due to diffusion or drift in the electrical field

Diffusion

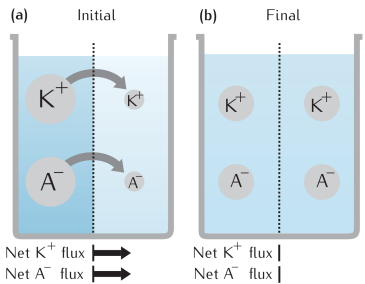

Electrodiffusion

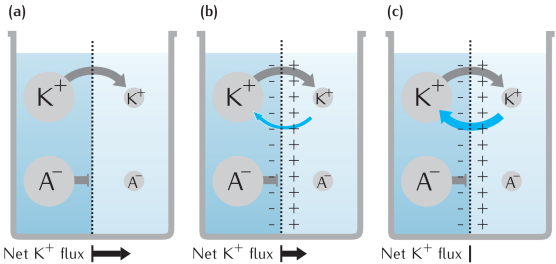

$$\mathbf{J}^k = \underbrace{-D^k \nabla [k]}_{\text{diffusion}}$$

$$\mathbf{J}_r^k = \underbrace{-D^k \nabla [k]}_{\text{diffusion}} \underbrace{- D^k \frac{z_k F}{RT} [k] \nabla \phi_r}_{\text{electrical drift}}.$$

Ions are conserved within each region and move due to diffusion or drift in the electrical field (Nernst–Planck)

Let $c_r^k = c_r^k(x, t)$ denote the concentration of (ion) species k in compartment r. Conservation of ions in the bulk of each compartment yields:

$$\frac{\partial c_r^k}{\partial t} + \nabla \cdot \mathbf{J}_r^k = 0,$$

where the ion flux density is given by:

$$\mathbf{J}_r^k = \underbrace{-D_r^k \nabla c_r^k}_{\text{diffusion}} \underbrace{- D_r^k \frac{z_k F}{RT} c_r^k \nabla \phi_r}_{\text{electrical drift}}.$$

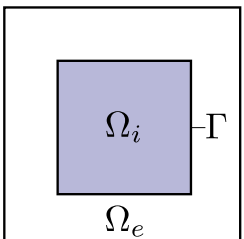

Tissue domain $\Omega = \Omega_i \cup \Omega_e \subset \mathbb{R}^d$, with (ion) species $k \in K$ (e.g. Na^+, K^+, Cl^-).

Ions are conserved within each region and move due to diffusion or drift in the electrical field (Nernst–Planck)

Let $c_r^k = c_r^k(x,t)$ denote the concentration of (ion) species k in compartment r. Conservation of ions in the bulk of each compartment yields:

$$\frac{\partial c_r^k}{\partial t} + \nabla \cdot \mathbf{J}_r^k = 0,$$

where the ion flux density is given by:

$$\mathbf{J}_r^k = \underbrace{-D_r^k \nabla c_r^k}_{\text{diffusion}} \underbrace{- D_r^k \frac{z_k F}{RT} c_r^k \nabla \phi_r}_{\text{electrical drift}}.$$

$2|K| + 2$ unknowns, but only $2|K|$ equations:

- Poisson–Nernst–Planck (PNP)
- Kirchhoff–Nernst–Planck (KNP)

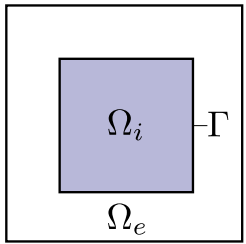

Tissue domain $\Omega = \Omega_i \cup \Omega_e \subset \mathbb{R}^d$, with (ion) species $k \in K$ (e.g. Na^+, K^+, Cl^-).

A charge imbalance in the ECS will typically vanish within nanoseconds

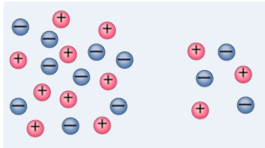

t = 0

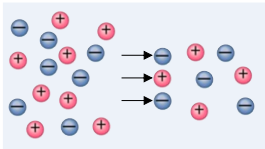

t < 10 ns

$D_{Cl^-} > D_{Na^+}$: Diffusion give net $(-)$ charge transport from left to right.

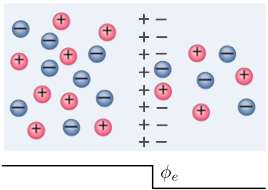

t > 10 ns

Quasi steady state: the potential ϕ_e prevents further charge separation.

A charge imbalance in the ECS will typically vanish within nanoseconds

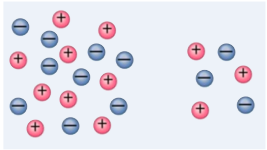

t = 0

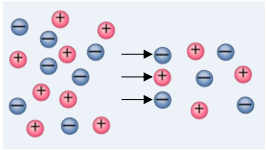

t < 10 ns

$D_{Cl^-} > D_{Na^+}$: Diffusion give net $(-)$ charge transport from left to right.

Poisson–Nernst–Planck (PNP):

$$\nabla^2 \phi_r = \frac{-\rho_r}{\epsilon_r}, \quad \rho_r = F \sum_k z_k [k]_r.$$

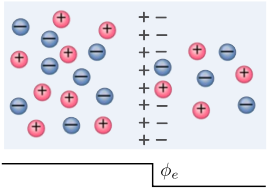

t > 10 ns

Quasi steady state: the potential ϕ_e prevents further charge separation.

Kirchhoff–Nernst–Planck (KNP):

$$\frac{\partial \rho_r}{\partial t} = 0, \quad \rho_r = F \sum_k z_k [k]_r.$$

The electroneutrality condition (KNP) is a good approximation on spatiotemporal scales larger than $\sim$ nanoseconds / nanometers

Poisson–Nernst–Planck (PNP)

Explicit modelling of charge relaxation processes - requires fine resolution

[Lopreore et al., 2008]

[Pods et al., 2013]

[Holcman and Yuste, 2015]

[Cartailler et al., 2017, 2017]

[Sacco et al., 2017]

Kirchhoff–Nernst–Planck (KNP)

Electroneutrality assumption - good approximation on larger scales ($>$ nano)

[Mori, 2009]

[Ellingsrud et al., 2020]

The KNP-EMI model

A computational framework for ionic electrodiffusion in brain tissue with explicit representation of the cells (KNP-EMI)

Consider a (tissue) domain $\Omega = \Omega_i \cup \Omega_e \subset \mathbb{R}^d$, where Ω_i (with boundary Γ) and Ω_e represent respectively intracellular and extracellular regions, with (ion) species $k \in K$ (e.g. Na^+, K^+, Cl^-).

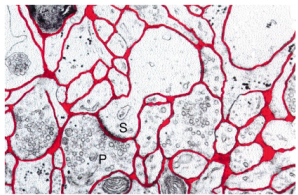

Rat cortex with ECS in red [Nicholson, 1998]

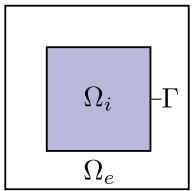

A computational framework for ionic electrodiffusion in brain tissue with explicit representation of the cells (KNP-EMI)

For each ion species $k \in K$, find the *ion concentrations* $c_r^k : \Omega_r \times (0, T] \to \mathbb{R}$ (mol/m^3) and the *electrical potentials* $\phi_r : \Omega_r \times (0, T] \to \mathbb{R}$ (V) such that:

$$\frac{\partial c_r^k}{\partial t} + \nabla \cdot \mathrm{J}_r^k = 0 \qquad \text{in } \Omega_r, \tag{6}$$

$$-F \sum_k z^k \nabla \cdot \mathrm{J}_r^k = 0 \qquad \text{in } \Omega_r, \tag{7}$$

for $r = \{i, e\}$, where the ion flux densities are given by:

$$\mathrm{J}_r^k = -D_r^k \nabla c_r^k - z^k \psi^k c_r^k \nabla \phi_r, \qquad \text{in } \Omega_r. \tag{8}$$

The system remains to be closed by appropriate initial conditions, boundary conditions, and importantly interface conditions.

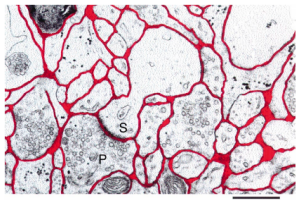

Rat cortex with ECS in red [Nicholson, 1998]

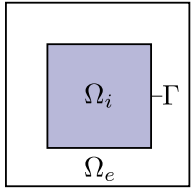

A computational framework for ionic electrodiffusion in brain tissue with explicit representation of the cells (KNP-EMI)

At the interface Γ, apply the following coupling conditions, and find the *total ionic current density* $I_M : \Gamma \times (0, T] \to \mathbb{R}$ (cm/m^{2}s) such that:

$$\phi_i - \phi_e = \phi_M, \qquad \text{on } \Gamma, \quad (9)$$

$$\frac{\partial \phi_M}{\partial t} = \frac{1}{C_M}(I_M - \sum_{k \in K} I_{\text{ion}}^k), \qquad \text{on } \Gamma, \quad (10)$$

$$I_M \equiv F \sum_k z^k \mathbf{J}_i^k \cdot n_i = -F \sum_k z^k \mathbf{J}_e^k \cdot n_e, \qquad \text{on } \Gamma, \quad (11)$$

$$\mathbf{J}_i^k \cdot n_i = \frac{I_{\text{ion}}^k + \alpha_i^k I_{\text{cap}}}{F z^k}, \qquad \text{on } \Gamma, \quad (12)$$

$$-\mathbf{J}_e^k \cdot n_e = \frac{I_{\text{ion}}^k + \alpha_e^k I_{\text{cap}}}{F z^k}, \qquad \text{on } \Gamma. \quad (13)$$

The transmembrane ion fluxes $I_{\text{ion}}^k = I_{\text{ion}}^k(\phi_M, [k], s)$ are subject to modelling, and may depend on gating variables governed by ODEs.

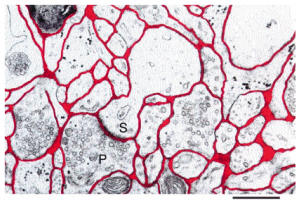

Rat cortex with ECS in red [Nicholson, 1998]

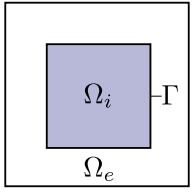

The strongly coupled and non-linear KNP-EMI equations set a rich scene for numerical exploration and can be solved in a multitude of ways

Numerical strategy:

- Split PDEs from ODEs (two-step first order)
- Finite difference ODE and PDE time discretizations (explicit handling of non-linear terms)
- Two different finite element based spatial discretization schemes:

Multi-dimensional form with mortar elements

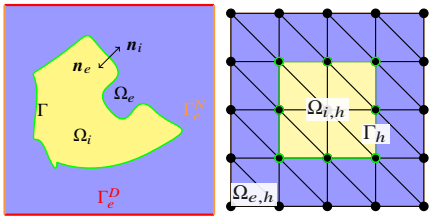

Single-dimensional form with DG elements

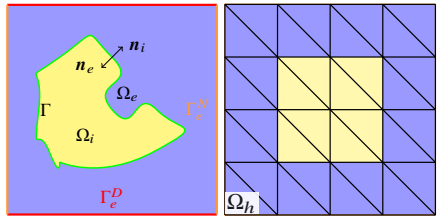

[Illustrations taken from Tveito et al. 2021. Modeling Excitable Tissue: The EMI Framework, chapter 5, Springer Nature]

We discretize the PDEs in space using a multi-dimensional formulation and mortar finite element spaces

Continuous form

The jumps across the interface Γ hinders us from defining global, differentiable concentrations and potentials in $H^1(\Omega)$. We instead seek for each r:

$$c_r^k \in H^1(\Omega_r), \quad \phi_r \in H^1(\Omega_r), \quad I_M \in H^1(\Gamma).$$

At each time step, find c_i^k, $\phi_i : \Omega_i \to \mathbb{R}$, c_e^k, $\phi_e : \Omega_e \to \mathbb{R}$ and $I_M : \Gamma \to \mathbb{R}$ such that:

$$\begin{bmatrix} \partial_t - \Delta & \pm\Delta & \pm\epsilon & & \\ \pm\Delta & -\Delta & -I & & \\ & I & -I & I & \\ & & -I & -\Delta & \pm\Delta \\ & & \pm\epsilon & \pm\Delta & \partial_t - \Delta \end{bmatrix} \begin{bmatrix} c_i^k \\ \phi_i \\ I_M \\ \phi_e \\ c_e^k \end{bmatrix} = f$$

Different variational problems posed over non-overlapping domains.

Spatial discretization

We discretize in space using a mortar finite element method:

$$c_{r,h}^k \in V_{r,h}, \quad \phi_{r,h} \in T_{r,h}, \quad I_{M,h} \in S_h,$$

where $V_{r,h}$, $T_{r,h}$, S_h are constructed using continuous piecewise linear polynomials.

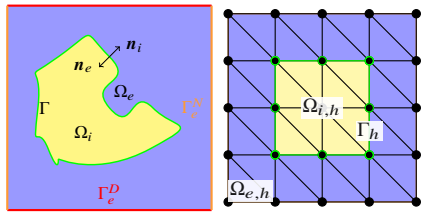

[$\Omega_{e,h}$ and $\Omega_{i,h}$ have identical facets on Γ, and the facets define the finite element cells of Γ_h.]

Implementing the system requires finite element software with mixed dimensional functionality

For a problem with a smooth manufactured solution we observe expected convergence rates.

$$c_i^{\mathrm{Na}} = 0.7 + 0.3\sin(2\pi x)\sin(2\pi y)(1 + e^{-t}),$$
$$c_e^{\mathrm{Na}} = 1.0 + 0.6\sin(2\pi x)\sin(2\pi y)(1 + e^{-t}),$$
$$\phi_e = cos(2\pi x)cos(2\pi y); \phi_i = \phi_e(1 + e^{-t}),$$
$$\dots$$

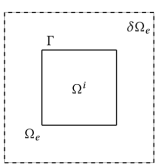

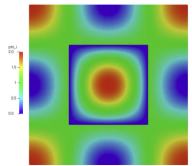

FENICS PROJECT

[Daversin-Catty, et al. 2021. Abstractions and automated algorithms for mixed domain finite element methods. TOMS]

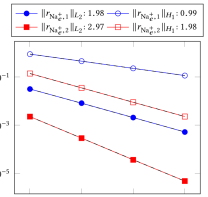

(a) Convergence study - Na_e^+

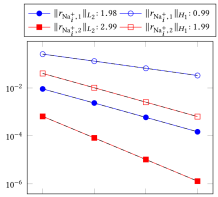

(b) Convergence study - Na_i^+

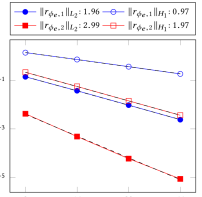

(c) Convergence study - ϕ_e

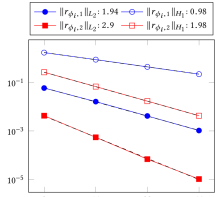

(d) Convergence study - ϕ_i

Alternatively, we can consider a single-dimensional formulation for the PDEs, discretized with DG elements

Single-dimensional form

- We eliminate the unknown $I_M : \Gamma \to \mathbb{R}$.
- We seek global concentrations and potentials:

$$c^k \in H^1(\cup_r \Omega_r), \quad \phi \in H^1(\cup_r \Omega_r),$$

belonging to the broken H^1 space $H^1(\cup_r \Omega_r) := \{u \in L^2(\Omega_r) : u|_{\Omega_r} \in H^1(\Omega_r), r \in \{i, e\}\}$.

Splitting scheme

- Split the equations for the concentrations and the potential and obtain two smaller, and more standard, sub-problems.

DG finite element discretization

Look for approximations in broken polynomial spaces for $k \geq 1$:

$$V_h^k(\mathcal{E}_h) = \{v \in L^2(\Omega) : v|_E \in P^k(E), \forall E \in \mathcal{E}_h\},$$

where $P^K(E)$ is the space of polynomials with total degree less than or equal to k.

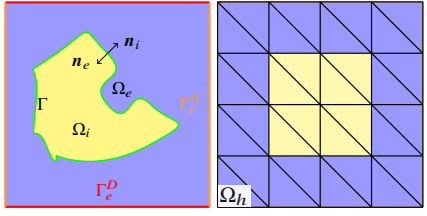

[Illustration taken from Tveito et al. 2021. Modeling Excitable Tissue: The EMI Framework, chapter 5, Springer Nature]

We apply a splitting scheme to obtain two smaller, and importantly more standard, sub-problems

Consider $n \in [1, \ldots, N]$ with t_n and assume that c^k_{n-1} at time step t_{n-1} are known.

Step I: Find $\phi_n \in H(\Omega)$ s.t.:

$$-F \sum_{k \in K} z^k \nabla \cdot \mathrm{J}^k(\phi_n, c^k_{n-1}) = 0, \tag{14}$$

$$\mathrm{J}^k(\phi_n, c^k_{n-1}) = -D^k \nabla c^k_{n-1} - z^k \psi^k c^k_{n-1} \nabla \phi_n. \tag{15}$$

Step II: Given ϕ_n (solution from Step I), find c^k_n for $k \in K$ such that:

$$\frac{\partial c^k_n}{\partial t} + \nabla \cdot \mathrm{J}^k(\phi_n, c^k_n) = 0, \tag{16}$$

$$\mathrm{J}^k(\phi_n, c^k_n) = -D^k \nabla c^k_n - z^k \psi^k c^k_n \nabla \phi_n. \tag{17}$$

We apply a splitting scheme to obtain two smaller, and importantly more standard, sub-problems

Consider $n \in [1, \ldots, N]$ with t_n and assume that c_{n-1}^k at time step t_{n-1} are known.

Step I: Find $\phi_n \in H(\Omega)$ s.t.:

$$-F \sum_{k \in K} z^k \nabla \cdot \mathrm{J}^k(\phi_n, c_{n-1}^k) = 0, \tag{14}$$

$$\mathrm{J}^k(\phi_n, c_{n-1}^k) = -D^k \nabla c_{n-1}^k - z^k \psi^k c_{n-1}^k \nabla \phi_n. \tag{15}$$

Insert (15) into (14) and we obtain:

$$\nabla \cdot (\kappa \nabla \phi_n) = f, \quad \kappa = F \sum_{k \in K} {z^k}^2 \psi^k c_{n-1}^k. \tag{18}$$

Step II: Given ϕ_n (solution from Step I), find c_n^k for $k \in K$ such that:

$$\frac{\partial c_n^k}{\partial t} + \nabla \cdot \mathrm{J}^k(\phi_n, c_n^k) = 0, \tag{16}$$

$$\mathrm{J}^k(\phi_n, c_n^k) = -D^k \nabla c_n^k - z^k \psi^k c_n^k \nabla \phi_n. \tag{17}$$

Insert (17) into (16) and we obtain:

$$\frac{\partial c_n^k}{\partial t} - \nabla \cdot (D^k \nabla c_n^k) - \nabla \cdot (z^k \psi^k c_n^k \nabla \phi_n) = 0. \tag{19}$$

We apply a splitting scheme to obtain two smaller, and importantly more standard, sub-problems

Consider $n \in [1, \ldots, N]$ with t_n and assume that c_{n-1}^k at time step t_{n-1} are known.

Step I: Find $\phi_n \in H(\Omega)$ s.t.:

$$-F \sum_{k \in K} z^k \nabla \cdot \mathrm{J}^k(\phi_n, c_{n-1}^k) = 0, \tag{14}$$

$$\mathrm{J}^k(\phi_n, c_{n-1}^k) = -D^k \nabla c_{n-1}^k - z^k \psi^k c_{n-1}^k \nabla \phi_n. \tag{15}$$

Insert (15) into (14) and we obtain:

$$\nabla \cdot (\kappa \nabla \phi_n) = f, \quad \kappa = F \sum_{k \in K} z^{k^2} \psi^k c_{n-1}^k. \tag{18}$$

Step II: Given ϕ_n (solution from Step I), find c_n^k for $k \in K$ such that:

$$\frac{\partial c_n^k}{\partial t} + \nabla \cdot \mathrm{J}^k(\phi_n, c_n^k) = 0, \tag{16}$$

$$\mathrm{J}^k(\phi_n, c_n^k) = -D^k \nabla c_n^k - z^k \psi^k c_n^k \nabla \phi_n. \tag{17}$$

Insert (17) into (16) and we obtain:

$$\frac{\partial c_n^k}{\partial t} - \nabla \cdot (D^k \nabla c_n^k) - \nabla \cdot (z^k \psi^k c_n^k \nabla \phi_n) = 0. \tag{19}$$

+ Reduces system to two smaller, more standard problems
- Introduces constraint on time step Δt

The weak formulation is discretized using a DG finite element method

- Symmetric interior penalty (SIPG) for the EMI sub-problem (18)
- SIPG on diffusion term; upwinding on advection term for the diffusion advection sub-problem (19).

For a problem with a smooth manufactured solution we observe expected convergence rates.

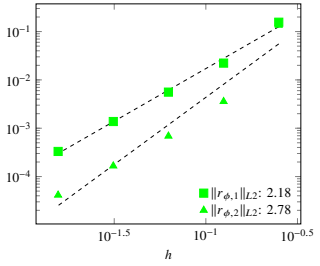

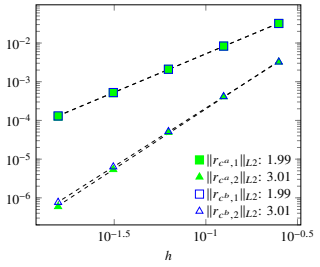

The weak formulation is discretized using a DG finite element method

- Symmetric interior penalty (SIPG) for the EMI sub-problem (18)
- SIPG on diffusion term; upwinding on advection term for the diffusion advection sub-problem (19).

For a problem with a smooth manufactured solution we observe expected convergence rates.

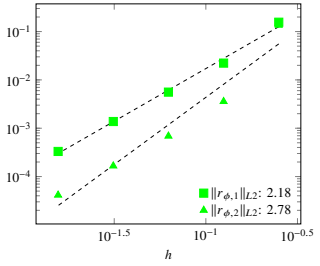

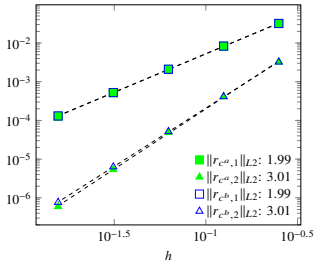

Ongoing work ...

- Peclet number in physiological scenarios?
- Robust preconditioners for the sub-problems?
- Stability and restriction on Δt in splitting scheme?

Comparing KNP-EMI and EMI

During hyperactivity, the KNP-EMI and EMI models differ due to shifts in the ion concentration gradients

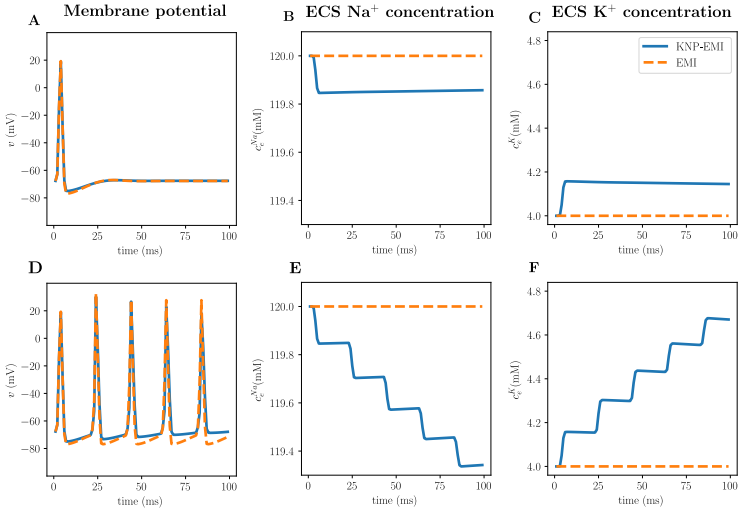

Normal activity (A, B, C):

- 1 Hz
- KNP-EMI and EMI give comparable results

Hyperactivity (D, E, F):

- 50 Hz
- Membrane potential predicted by KNP-EMI slightly (and persistently) depolarizes for each AP

During hyperactivity, the KNP-EMI and EMI models differ due to shifts in the ion concentration gradients

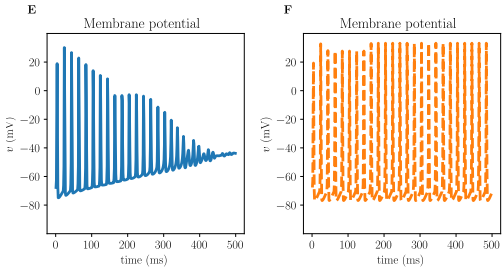

Normal activity (not shown):

- 1 Hz
- KNP-EMI and EMI give comparable results

Hyperactivity (E, F):

- 50 Hz
- Membrane potential predicted by KNP-EMI slightly (and persistently) depolarizes for each AP

A study of ephaptic coupling

Comparing KNP-EMI and EMI: Do diffusive currents affect ephaptic coupling through the ECS in unmyelinated axon bundles?

In an idealized axon bundle with cell gaps of 0.1μm, action potentials are induced (via a synaptic current) every 20 seconds in either:

- Axon A (1 active neighbour), or
- Axons B and C (8 active neighbour).

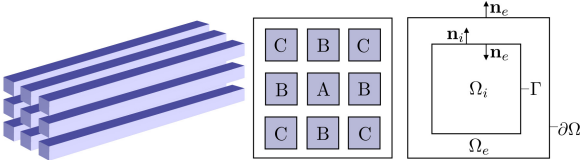

[Ellingsrud et al., 2020]

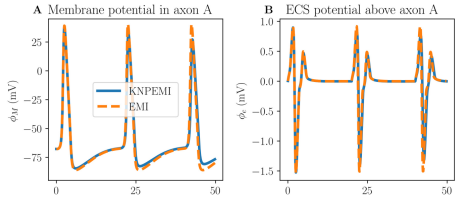

Diffusive currents contribute to ECS potential shifts in the KNP-EMI framework:

EMI $\quad \nabla \cdot (\sigma_e \nabla \phi_e) = 0, \text{ in } \Omega_e,$

KNP-EMI $\quad \nabla \cdot (\sigma_e \nabla \phi_e + \nabla b_e) = 0, \text{ in } \Omega_e,$

where $b_e = F \sum_k z^k D_e^k [k]_e$.

Diffusive currents do not strengthen the *electrical* ephaptic coupling (via the extracellular potential), however we see *diffusive* ephaptic coupling

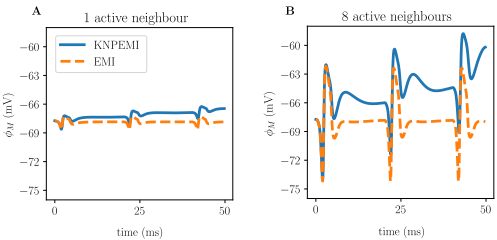

Diffusive currents do not strengthen the *electrical* ephaptic coupling (via the extracellular potential), however we see *diffusive* ephaptic coupling

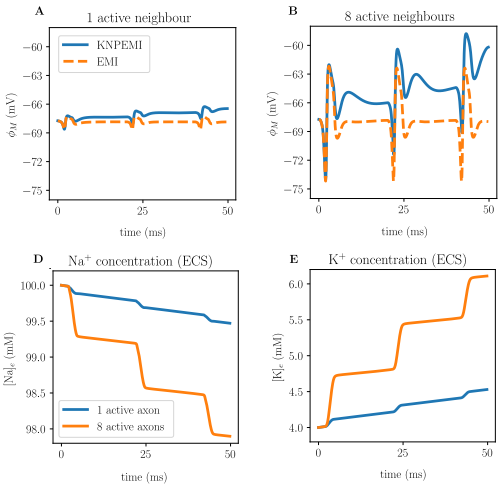

Diffusive currents do not strengthen the *electrical* ephaptic coupling (via the extracellular potential), however we see *diffusive* ephaptic coupling

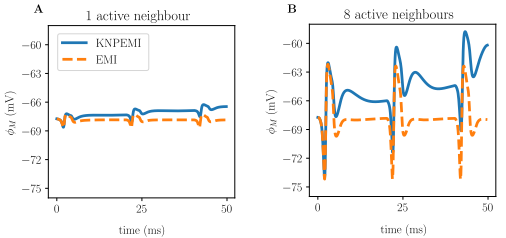

Ephaptic coupling is inversely proportional to the extracellular conductivity:

$$\sigma_i = \frac{F}{\psi}\sum_k D_i^k [k]_i (z^k)^2 = 2.01 \qquad \sigma_i = 1.0,\ \text{(S/m)}$$

$$\sigma_e = \frac{F}{\psi}\sum_k D_e^k [k]_e (z^k)^2 = 1.31 \qquad \sigma_e = 0.1,\ \text{(S/m)}$$

[Bokil et al., 2001]

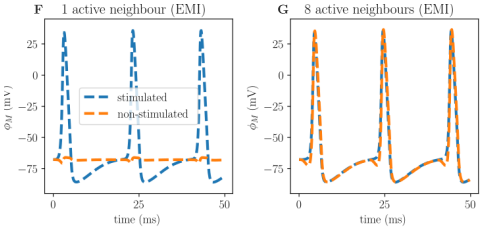

Future perspectives

Exciting times: Extreme modelling of excitable tissue

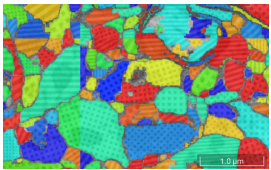

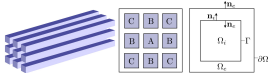

EMIx

The Research Council of Norway

Ambition

To establish mathematical and technological foundations for modelling and simulation of electrical, chemical and mechanical interplay between brain cells at unprecedented detail, allowing for pioneering in-silico studies of brain signalling, volume balance and clearance.

Topics and expected outcomes

- Well-posed general mathematical and numerical framework allowing for geometrically-explicit representations of moving excitable cells;
- New computational geometries and models, highly scalable algorithms, and solution software for high-resolution high-realism simulations of excitable cell ensembles – all distributed as open source;
- New physiological insight into inter-neuronal and astrocyte membrane mechanisms and their role in brain homeostasis and learning.

Funding

Research Council of Norway, FRIPRO (12 MNOK, 2021–2025)

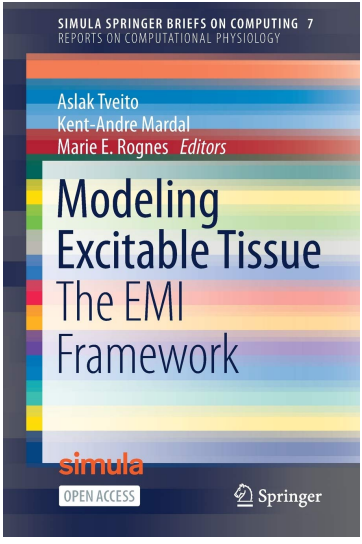

Collaborators: Cécile Daversin-Catty, Gaute Einevoll, Geir Halnes, Miroslav Kutcha, Rami Masri, Marie Rognes, Andreas Solbrå.

KNP-EMI paper: https://doi.org/10.3389/fninf.2020.00011

Modeling Excitable Tissue - The EMI Framework: https://doi.org/10.1007/978-3-030-61157-6

Abstractions and automated algorithms for mixed domain finite element methods: https://doi.org/10.1145/3471138

This research is supported by the European Research Council (ERC) under the European Union's Horizon 2020 research and innovation programme under grant agreement 714892 (Waterscales) and by the Research Council of Norway via FRIPRO grant agreement 324239 (EMIx).